Contrib. Astron. Obs. Skalnaté Pleso **53**/**4**, 164 – 174, (2023)
https://doi.org/10.31577/caosp.2023.53.4.164

Investigating star formation in nearby interacting galaxies

A.P. Joó, B. Koncz and E. Pichler

Eötvös Loránd University, Hungary

Received: June 30, 2023; Accepted: October 10, 2023

Abstract. We are investigating how the interaction between galaxies in the local Universe triggers star formation, both globally and in different regions of the galaxies. We highlight two examples where one of the interacting galaxies is significantly smaller. We look at combined spectrographic and multi-wavelength photometric data to look for tracers of intense star formation and obtain metallicities. Comparing the calculated star formation surface densities and metallicities to isolated galaxies gives us a hint at how star formation and the composition of the interstellar material evolved through the interaction. Resolving the nearby galaxies shows how differently the two galaxies change due to the interaction, and at the same time, it makes it possible to identify local star-forming regions with different characteristics.

Key words: Galaxies: interactions – Galaxies: ISM – Galaxies: star formation

1. Introduction

Star formation plays a key role in the chemical evolution of galaxies, and through that, primarily influences the chemical composition of the Universe. High-mass star formation contributes to this process most significantly, as most of the chemical elements are only produced in supernovae (SN) explosions at the end of high-mass stars' evolution.

The environment suitable for high-mass star formation has to contain a high amount of cold interstellar material (ISM) in a compact region of space, in the form of a gravitationally bound giant molecular cloud (GMC) containing (mostly Hydrogen-) gas and dust with a mass of at least $10^4 M_{Sun}$. As a consequence, star formation and high-mass star formation, in particular, occurs in regions partly or fully obscured by dust, in some cases hiding the entire galaxy, see eg. the so-called dust-obscured galaxies (Suleiman et al., 2022).

Usually, only large spiral galaxies contain a large number of GMCs that can fuel a high rate of star formation or even a starburst episode in the galaxy. Merger events, however, provide a possibility for smaller galaxies to acquire enough material to be able to host high-mass star formation. In these cases, the material gain is usually localized in the interacting region between the galaxies, and limited to the time of the interaction. To study these cases, the observation

of nearby, resolved galaxy interactions is required. Nearby galaxies are also of great interest in multimessenger gravitational wave - gamma-ray burst (GW-GRB) detections which are also connected to high-mass star formation (see e.g. the first multimessenger GW-GRB detections Abbott et al. (2017), Goldstein et al. (2017), Bagoly et al. (2016), Horváth et al. (2018), Tóth et al. (2019)).

We investigated two nearby galaxy interactions: M51 and Arp 84 using archival and literature data. We focused on the star formation rate and the chemical composition of different regions of the galaxy pairs. A typical method to estimate the physical parameters of the star-forming cold ISM in galaxies up to large distances is observing CO lines (see eg. Hatsukade et al. (2019)). Star formation may also be traced by PAH emission (see eg. Kovács et al. (2019)). A linear relationship was found by eg. Liu et al. (2016) between star formation rate and dust continuum emission for both Galactic clumps and the high redshift ($z > 1$) star-forming galaxies, indicating a constant gas depletion time of 100 Myr for molecular gas. Therefore we used Hα intensity maps and spectral data with star formation tracing line ratios as star formation rate indicators, CO line maps for mapping molecular clouds, and X-ray intensity maps as indicators for high-mass star formation.

The layout of this paper is as follows: in Section 2 and 3 we show our analysis of the two galaxy interactions, then we sum up our findings in Section 4.

2. M51

M51 (Fig. 1) is an interacting galaxy pair consisting of a larger spiral NGC 5194 (M51a) and a smaller, dusty spheroid NGC 5195 (M51b), in the constellation

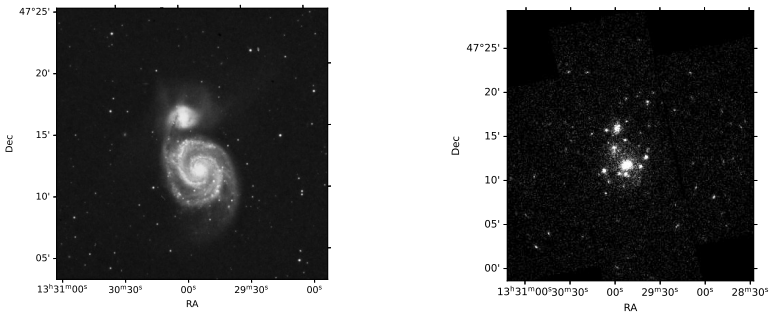

Figure 1. M51 Galaxy pair: NGC 5194 (M51a) spiral galaxy and its dusty spheroid companion NGC 5195 (M51b). **a)** Left: Palomar Observatory optical image, 48-inch Schmidt Telescope, 645 nanometer, **b)** Right: XMM Newton X-ray image, EPIC MOS camera, 0.15 - 15 keV

Canes Venatici, at a distance of 7.9 Mpc according to Wei et al. (2020).

Previous works report a roughly Solar metallicity for NGC 5194 (Bresolin et al. 2004, Walter et al. 2008) with a relatively flat gradient (Bresolin et al., 2004). Walter et al. (2008) calculated a star formation rate of $6.05 M_{Sun}/yr$ for NGC 5194, and Lee et al. (2011) and Lee et al. (2012) found that the two galaxies have very different star formation rates. The larger spiral NGC 5194 is gas-rich, while its companion is gas-poor (Watkins et al. 2015).

We are interested in the distribution and chemical composition of the star-forming regions in M51. We are focusing on the interacting region between the two galaxies, in order to see how it affects star formation activity and chemical composition.

The spiral arm of NGC 5194 between the two galaxy centers seems to contain mostly sub-solar metallicity areas, some with high star-formation rate surface density (Wei et al., 2020). We analyzed the metallicity (Oxygen abundance) and the star formation rate surface density (Σ_{SFR}) of 113 regions observed by Wei et al. (2020), each with a diameter of about 75 pc. In particular, we were interested in finding correlations of the parameters, as well as any clustering of the data points.

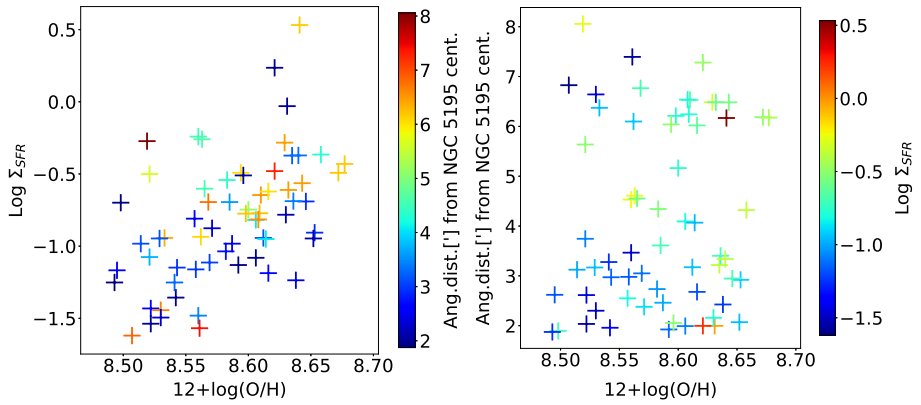

Figure 2. Properties of selected 75 pc diameter areas in M51 from Wei et al. (2020). **a)** Left: Σ_{SFR} with respect to metallicity. The color scale shows the distance from the center of NGC 5195. A linear correlation can be seen between star formation and metallicity with a coefficient of 0.51. **b)** Right: Angular distance with respect to metallicity. The color scale shows the Σ_{SFR} of the areas. A higher fraction of areas with lower star formation rates can be seen closer to the center of NGC 5195.

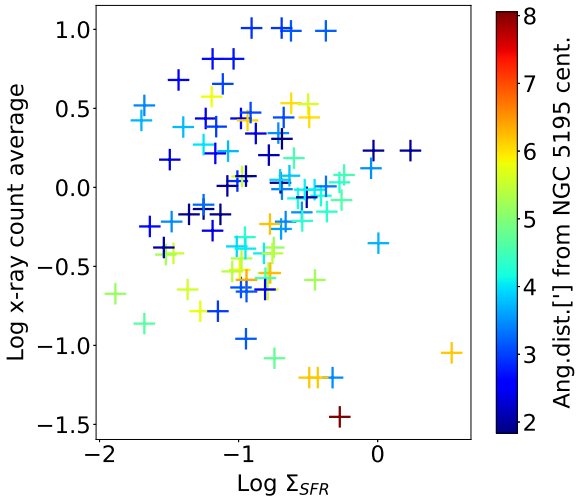

Figure 3. The average X-ray instrumental flux of 75 pc diameter areas in M51 with respect to the Σ_{SFR}. The color scale shows the angular distance from the center of NGC 5195. A slight correlation between the X-ray flux and the Σ_{SFR} can be seen with $PCC = 0.11$, and two groups are separatable by the distance from the center of NGC 5194.

Fig. 2a) shows the Σ_{SFR} with respect to the metallicity, with the color scale showing the distance from the center of NGC 5195, the smaller, spherical galaxy. We found a linear correlation between the metallicity and the Σ_{SFR} with Pearson correlation coefficient $PCC = 0.51$. The interacting region is between 2-3 arcminutes in distance, areas here show diversity, while areas further away tend to group around higher metallicities with a few exceptions.

Fig. 2b) displays the distance from the center of NGC 5195 with respect to the metallicity, with the colors showing Σ_{SFR} this time. The scarce region between 4 and 6 arcmin distance corresponds to the gap between the inner and outer arm of NGC 5194 in the south-eastern direction. We see a higher fraction of areas with lower star formation rates closer to the center of NGC 5195.

Both plots reinforce the basic concept of the larger spiral galaxy having higher star formation activity, which leads to higher metallicities, but at the same time, a notable amount of areas can be found in the interacting region with high star formation activity and corresponding high metallicities, the formation of which could most probably be attributed to the interaction between the two galaxies.

As there is an established connection between the star formation rate and the X-ray flux (for example Grimm et al. (2003), Mineo et al. (2012)), of which

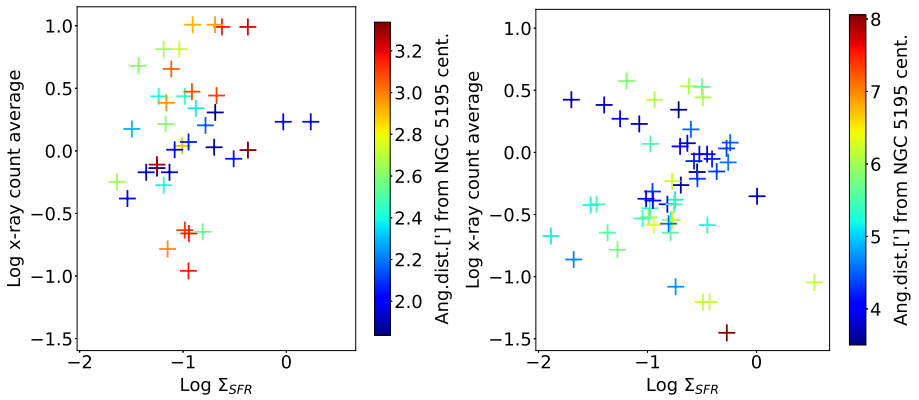

Figure 4. The average X-ray instrumental flux of 75 pc diameter areas in M51 with respect to the Σ_{SFR}. The color scale shows the angular distance from the center of NGC 5195. The two plots show two groups separated by the distance from the center of NGC 5195. Left: areas closer to the center of NGC 5195, mostly in the interacting region. Right: areas mostly outside the interacting region in NGC 5194. Please note, that the same color scale shows different values in the two plots. Areas in the interacting region have higher X-ray fluxes in general.

about 66% comes from X-ray binaries and the rest mostly from hot ISM (Mineo et al., 2013), we used the X-ray flux as a traces for high-mass star formation and looked at its the distribution in M51.

For calculating X-ray flux we used an XMM Newton X-ray image taken with the EPIC MOS camera in the energy range from 0.15 to 15 keV. We calculated average instrumental fluxes for the areas measured by Wei et al. (2020) with the background noise subtracted. We then compared the X-ray fluxes to the Σ_{SFR} and metallicity of the measured areas to see correlations.

You can see our comparison in Fig. 3. There is a slight overall correlation between the X-ray flux and the Σ_{SFR} with $PCC = 0.11$, and two groups can be separated by distance from the center of NGC 5195, which we show in Fig. 4.

The areas closer to the center of NGC 5195 (up to a distance of ≈3.5 arcminutes) are mostly in the interacting region, while the other areas are mostly outside of the interacting region in NGC 5194. The closer areas have higher X-ray flux on average, however, the dispersion is significant, which we attribute to the turbulent nature of the interaction. These findings support the hypothesis of the interacting region having a higher rate of high-mass star formation, which

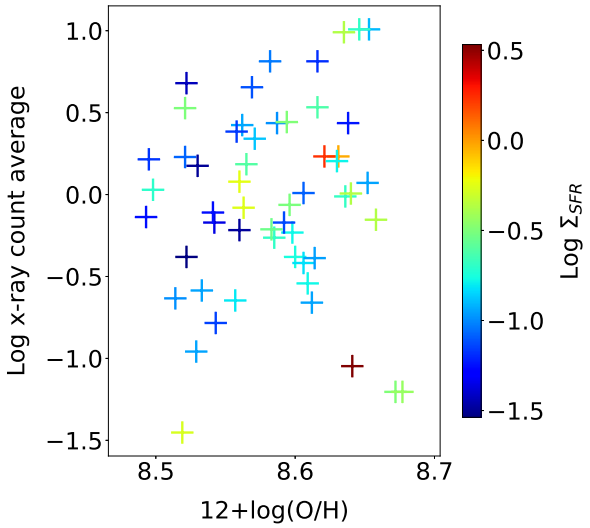

Figure 5. X-ray instrumental flux of 75 pc diameter areas in M51 with respect to the metallicity. The color scale shows the Σ_{SFR}. No correlation can be seen with $PCC = -0.07$.

could be the cause of the higher density and pressure of colliding interstellar material in this region.

We also looked at how the X-ray flux changes with respect to the metallicity, as seen in Fig. 5, which shows no correlation ($PCC = -0.07$).

3. Arp84

Arp 84 is a strongly interacting galaxy pair also in the constellation of Canis Venatici at a distance of 50 Mpc (Smith et al., 2007) consisting of a larger spiral NGC 5395 and a smaller spiral NGC 5394 (see Fig. 6).

Examining the CALIFA[1] spectroscopic data for NGC 5394, the smaller galaxy of the pair, Roche et al. (2015) calculated a star formation rate of 3.39 M_{Sun}/yr, and an oxygen abundance $log(O/H) + 12 \approx 8.6$ which corresponds to 0.76 Solar metallicity.

The Arp 84 galaxy pair is significantly less resolved than M51, but still suitable for the purpose of our analysis of the distribution of star-forming regions and their chemical composition.

[1]Calar Alto Legacy Integral Field Area survey, optical integral-field spectroscopy (Sánchez, S. F. et al., 2012)

Roche et al. (2015) found that most of the star-forming activity is concentrated at the nucleus (75% in the central r $<$ 1 kpc) which is most probably driven by AGN activity. Additional star-forming regions can be found in the interacting region, the SW part of the disk, and in two hot spots on the northern tidal arm. Furthermore, the outer tidal arms have a post-starburst spectrum, evidence of a more intensive star formation episode a few $\cdot 10^8$ years ago. The CALIFA data also show an annular region at radii 2.25 - 4 kpc from the nucleus, with elevated ratios of [NII], [OI]6300 to the Balmer lines - this is evidence of shock excitation, which might be the result of interaction-triggered gas inflow.

Kaufman et al. (1999) also notes that while NGC 5394's CO emission mostly comes from the central starburst region, it has a lopsided gas distribution in the disk with more CO, Hα, and HI emission from the western or southwestern side.

These findings support the presence of elevated star formation activity in the interacting region with a generally subsolar metallicity. In order to further test this, we analyzed Herschel PACS[2] 70-micron infrared data from the Herschel Science Archive.

We determined the positions of clumps on the Arp 84 70 micron infrared image (see Fig. 7) and calculated their distances from the center of NGC 5394, the smaller galaxy of the interacting pair. We then calculated the average intensities for the selected areas and subtracted the RMS noise measured on the image backgrounds. For the diameter of the areas, we used a diameter of 30 arcseconds, corresponding to $\sim$7 kpc.

In the resulting Fig. 8, we see a strong correlation between the optical and the 70-micron instrumental flux with a coefficient of $PCC = 0.87$. The correlation is evident on the clumps with the closest (blue crosses) and farthest (red and

[2]Photodetector Array Camera and Spectrometer, one of the three science instruments on ESA's far infrared and submillimeter observatory. (Poglitsch, A. et al., 2010)

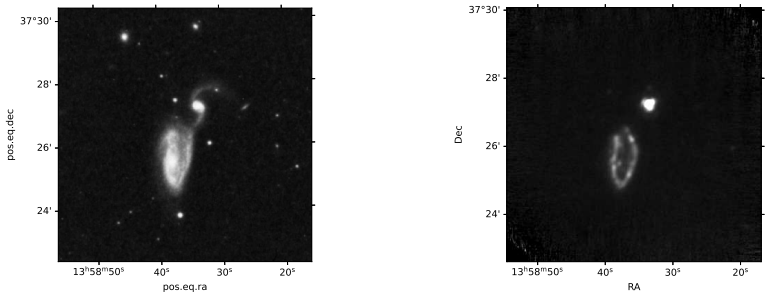

Figure 6. The Arp 84 interacting galaxy pair: NGC 5395 (the larger one) and NGC 5394. **a)** Left: Palomar Observatory optical image, 48-inch Schmidt Telescope, 645 nm. **b)** Right: Herschel PACS 70 micron image.

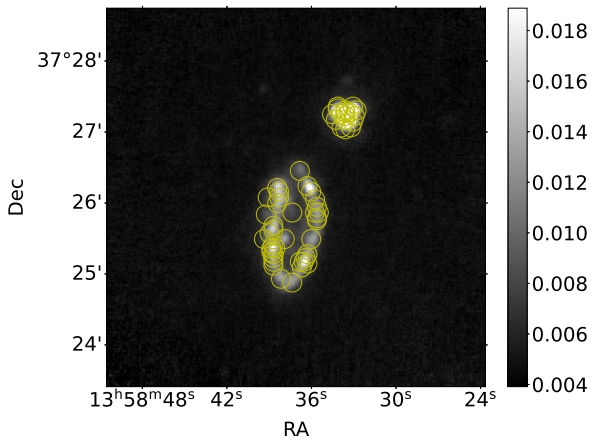

Figure 7. Selected areas of interest in Arp 84 on the Herschel PACS 70 micron image.

orange crosses) angular distance from the small galaxy's center. A few areas, however, between the distance of about 1 - 2 arcminutes (cyan crosses) seem to deviate to some extent from the trend. From these, the most interesting are the ones at around 1 arcminute distance from the lower mass galaxy, NGC5394. Those areas correspond to the interacting region, and apparently bright both in optical and FIR, with higher relative 70 micron fluxes, which could be a sign of (partly dust obscured) elevated star formation activity.

4. Summary

We analyzed the distribution and chemical composition of star formation regions in the two interacting galaxy pairs M51 and Arp 84. We found higher star formation rates in the interacting galaxies compared to field galaxies and a sub-solar average metallicity in the smaller galaxies. Tracers of star formation show areas in the interacting regions with elevated star formation activity, in some cases even starburst events. These findings present examples of the possibility, that galaxies with lower general metallicity can have areas with high star formation rates or even starburst episodes in merger events, which induces high-mass star formation as well.

Acknowledgements.

We are grateful to L. Viktor Tóth for his supervision of this work and to the High Energy Astronomy Research Team (HEART - https://physics.elte.hu/KRFT_heart) for their support and thoughtful feedback. We thank the anonymous referee for the careful reading of our manuscript and the valuable comments and suggestions.

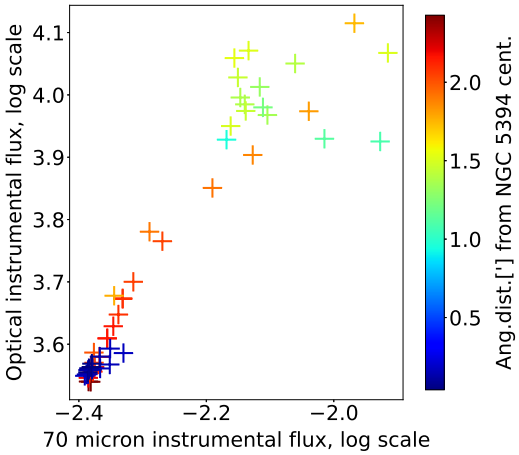

Figure 8. The average 70 micron instrumental flux of selected areas of interest in Arp 84 with respect to the average optical instrumental flux. The color scale shows the angular distance from the center of NGC 5394 (the smaller interacting galaxy). There is a strong correlation with a coefficient of $PCC = 0.87$.

The IBWS conference participation of B. Koncz was subsidized by the Talent Support Council of ELTE Eötvös Loránd University, Budapest. The authors thank for the Hungarian OTKA K-146092 grant.

References

Abbott, B. P., Abbott, R., Abbott, T. D., et al., GW170814: A Three-Detector Observation of Gravitational Waves from a Binary Black Hole Coalescence. 2017, *Physical Review Letters*, **119**, 141101, DOI: 10.1103/PhysRevLett.119.141101

Bagoly, Z., Szécsi, D., Balázs, L. G., et al., Searching for electromagnetic counterpart of LIGO gravitational waves in the Fermi GBM data with ADWO. 2016, *Astronomy and Astrophysics*, **593**, L10, DOI: 10.1051/0004-6361/201628569

Bresolin, F., Garnett, D. R., & Robert C. Kennicutt, J., Abundances of Metal-rich H ii Regions in M51*. 2004, *Astronomical Journal*, **615**, 228, DOI: 10.1086/424377

Goldstein, A., Veres, P., Burns, E., et al., An Ordinary Short Gamma-Ray Burst with Extraordinary Implications: Fermi-GBM Detection of GRB 170817A. 2017, *Astrophysical Journal, Letters*, **848**, L14, DOI: 10.3847/2041-8213/aa8f41

Grimm, H.-J., Gilfanov, M., & Sunyaev, R., High-mass X-ray binaries as a star formation rate indicator in distant galaxies. 2003, *Monthly Notices of the RAS*, **339**, 793, DOI: 10.1046/j.1365-8711.2003.06224.x

Hatsukade, B., Hashimoto, T., Kohno, K., et al., Molecular Gas Properties in the Host Galaxy of GRB 080207. 2019, *Astrophysical Journal*, **876**, 91, DOI: 10.3847/1538-4357/ab1649

Horváth, I., Tóth, B. G., Hakkila, J., et al., Classifying GRB 170817A/GW170817 in a Fermi duration-hardness plane. 2018, *Astrophysics and Space Science*, **363**, 53, DOI: 10.1007/s10509-018-3274-5

Kaufman, M., Brinks, E., Elmegreen, B. G., et al., The Interacting Galaxies NGC 5394/5395: A Post-Ocular Galaxy and Its Ring/Spiral Companion. 1999, *Astronomical Journal*, **118**, 1577, DOI: 10.1086/301030

Kovács, T. O., Burgarella, D., Kaneda, H., et al., Star formation and polycyclic aromatic hydrocarbons in ELAIS N1 galaxies as seen by AKARI. 2019, *Publications of the ASJ*, **71**, 27, DOI: 10.1093/pasj/psy145

Lee, J. H., Kim, S. C., Park, H. S., et al., HUBBLE SPACE TELESCOPE PIXEL ANALYSIS OF THE INTERACTING FACE-ON SPIRAL GALAXY NGC 5194 (M51A). 2011, *The Astrophysical Journal*, **740**, 42, DOI: 10.1088/0004-637X/740/1/42

Lee, J. H., Kim, S. C., Ree, C. H., et al., HUBBLE SPACE TELESCOPE PIXEL ANALYSIS OF THE INTERACTING S0 GALAXY NGC 5195 (M51B). 2012, *The Astrophysical Journal*, **754**, 80, DOI: 10.1088/0004-637X/754/2/80

Liu, T., Kim, K.-T., Yoo, H., et al., Star Formation Laws in Both Galactic Massive Clumps and External Galaxies: Extensive Study with Dust Coninuum, HCN (4-3), and CS (7-6). 2016, *Astrophysical Journal*, **829**, 59, DOI: 10.3847/0004-637X/829/2/59

Mineo, S., Gilfanov, M., Lehmer, B. D., Morrison, G. E., & Sunyaev, R., X-ray emission from star-forming galaxies – III. Calibration of the LX-SFR relation up to redshift z $\approx$ 1.3. 2013, *Monthly Notices of the RAS*, **437**, 1698, DOI: 10.1093/mnras/stt1999

Mineo, S., Gilfanov, M., & Sunyaev, R., X-ray emission from star-forming galaxies – I. High-mass X-ray binaries. 2012, *Monthly Notices of the RAS*, **419**, 2095, DOI: 10.1111/j.1365-2966.2011.19862.x

Poglitsch, A., Waelkens, C., Geis, N., et al., The Photodetector Array Camera and Spectrometer (PACS) on the Herschel Space Observatory*. 2010, *A&A*, **518**, L2, DOI: 10.1051/0004-6361/201014535

Roche, N., Humphrey, A., Gomes, J. M., et al., CALIFA spectroscopy of the interacting galaxy NGC 5394 (Arp 84): starbursts, enhanced [N ii]6584 and signs of outflows and shocks. 2015, *Monthly Notices of the RAS*, **453**, 2349, DOI: 10.1093/mnras/stv1669

Sánchez, S. F., Kennicutt, R. C., Gil de Paz, A., et al., CALIFA, the Calar Alto Legacy Integral Field Area survey - I. Survey presentation. 2012, *A&A*, **538**, A8, DOI: 10.1051/0004-6361/201117353

Smith, B. J., Struck, C., Hancock, M., et al., The Spitzer Spirals, Bridges, and Tails Interacting Galaxy Survey: Interaction-Induced Star Formation in the Mid-Infrared. 2007, *Astronomical Journal*, **133**, 791, DOI: 10.1086/510350

Suleiman, N., Noboriguchi, A., Toba, Y., et al., The statistical properties of 28 IR-bright dust-obscured galaxies and SED modelling using CIGALE. 2022, *Publications of the ASJ*, **74**, 1157, DOI: 10.1093/pasj/psac061

Tóth, B. G., Rácz, I. I., & Horváth, I., Gaussian-mixture-model-based cluster analysis of gamma-ray bursts in the BATSE catalog. 2019, *Monthly Notices of the RAS*, **486**, 4823, DOI: 10.1093/mnras/stz1188

Walter, F., Brinks, E., de Blok, W. J. G., et al., THINGS: The H I Nearby Galaxy Survey. 2008, *Astronomical Journal*, **136**, 2563, DOI: 10.1088/0004-6256/136/6/2563

Watkins, A. E., Mihos, J. C., & Harding, P., Deep Imaging of M51: A New View of The Whirlpool's Extended Tidal Debris. 2015, *Astrophysical Journal, Letters*, **800**, L3, DOI: 10.1088/2041-8205/800/1/L3

Wei, P., Zou, H., Kong, X., et al., Physical Properties of H ii Regions in M51 from Spectroscopic Observations. 2020, *Publications of the ASP*, **132**, 094101, DOI: 10.1088/1538-3873/ab9d92